Consistency of ARESE II cloud absorption estimates and sampling issues

L. Oreopoulos,[1,2] A. Marshak,[1,2] and R. F. Cahalan[2]

Received 26 February 2002; revised 12 August 2002; accepted 13 August 2002; published 15 January 2003.

[1] Data from three cloudy days (3, 21, and 29 March 2000) of the Atmospheric Radiation Measurement (ARM) Enhanced Shortwave Experiment II (ARESE II) were analyzed and broadband absorptances were obtained for three sets of instruments. Grand (total flight) averages of fractional solar absorptances were ~0.21–0.22, with the exception of 3 March when two sets of instruments gave values smaller by ~0.03–0.04. The robustness of these values was evaluated by examining potential sampling problems with the aid of 500 nm spectral fluxes. The grand average of 500 nm apparent absorptance was statistically indistinguishable from zero for 21 and 29 March but acquired a large positive value of ~0.10 on 3 March, which is not physically understood. We present results showing that each of the three days is unique in terms of cloud morphology and behavior of the absorptance time series. When the conditional sampling method is applied to the two days with reliable 500 nm absorptances (21 and 29 March), the resulting histogram of broadband absorptances is significantly narrower than the histogram constructed from the original time series. Corrections to the absorptance time series à la *Cess et al.* [1999] were successful for all three days because of the generally good correlation between broadband and 500 nm absorptances, removing the bulk of low-end and high-end extremes most likely associated with sampling and horizontal flux artifacts. The above two methods suggest an ARESE II range of broadband absorptances of ~0.18–0.26. Finally, our study shows that the data set obtained on 29 March is the most self-consistent and straightforward to analyze among the three, because this day fulfilled all the requirements of the ARESE II experimental design, namely the presence of thick, overcast, homogeneous clouds. *INDEX TERMS:* 0320 Atmospheric Composition and Structure: Cloud physics and chemistry; 3359 Meteorology and Atmospheric Dynamics: Radiative processes; 3360 Meteorology and Atmospheric Dynamics: Remote sensing; *KEYWORDS:* atmospheric absorption, cloud absorption, solar radiation, 3-D effects, sampling, horizontal flux

Citation: Oreopoulos, L., A. Marshak, and R. F. Cahalan, Consistency of ARESE II cloud absorption estimates and sampling issues, *J. Geophys. Res.*, *108*(D1), 4029, doi:10.1029/2002JD002243, 2003.

1. Introduction

[2] Recent efforts to resolve the controversial issue of modeled versus observed cloudy sky absorption included two field experiments in the vicinity of the Atmospheric Radiation Measurement (ARM) Program Oklahoma Southern Great Plains (SGP) instrument site. Both ARM Enhanced Shortwave Experiments (ARESE) had as a common goal to measure atmospheric absorption explicitly by taking the difference of observed net radiative fluxes at two height levels. ARESE I (which originally was simply called ARESE) took place from 22 September to 1 November 1995. The absorption of an atmospheric column extending from ~0.5 to ~13 km was obtained from fluxes measured by broadband and narrowband radiometers fitted on aircraft flying in coordination at these altitudes. Results from this experiment were documented extensively in the literature [e.g., *Cess et al.*, 1996; *Valero et al.*, 1997a, 1997b; *Zender et al.*, 1997; *Li et al.*, 1999; *O'Hirok et al.*, 2000]. According to some analyses, ARESE I indicated an increase in broadband absorptance with cloud fraction [*Cess et al.*, 1999], with values of ~0.13 for clear skies and ~0.32 for heavy overcast skies [*Valero et al.*, 2000]. The magnitude of observed cloudy sky absorptance was substantially higher than values estimated not only by the spectrally unsophisticated plane-parallel broadband radiation codes implemented in General Circulation Models (GCMs) [*Valero et al.*, 2000], but also a more detailed three-dimensional (3-D) spectral Monte Carlo code [*O'Hirok et al.*, 2000].

[3] ARESE II was conducted almost 5 years later, from 21 February to 15 April 2000 with the intention to focus on heavy stratus clouds. Due to budgetary constraints only one aircraft was employed, thus significantly departing from the experimental design of ARESE I. A Twin Otter aircraft flew

[1]Joint Center for Earth Systems Technology, University of Maryland Baltimore County (UMBC), Baltimore, Maryland, USA.
[2]Climate and Radiation Branch, National Aeronautics and Space Administration (NASA) Goddard Space Flight Center, Greenbelt, Maryland, USA.

0148-0227/03/2002JD002243$09.00

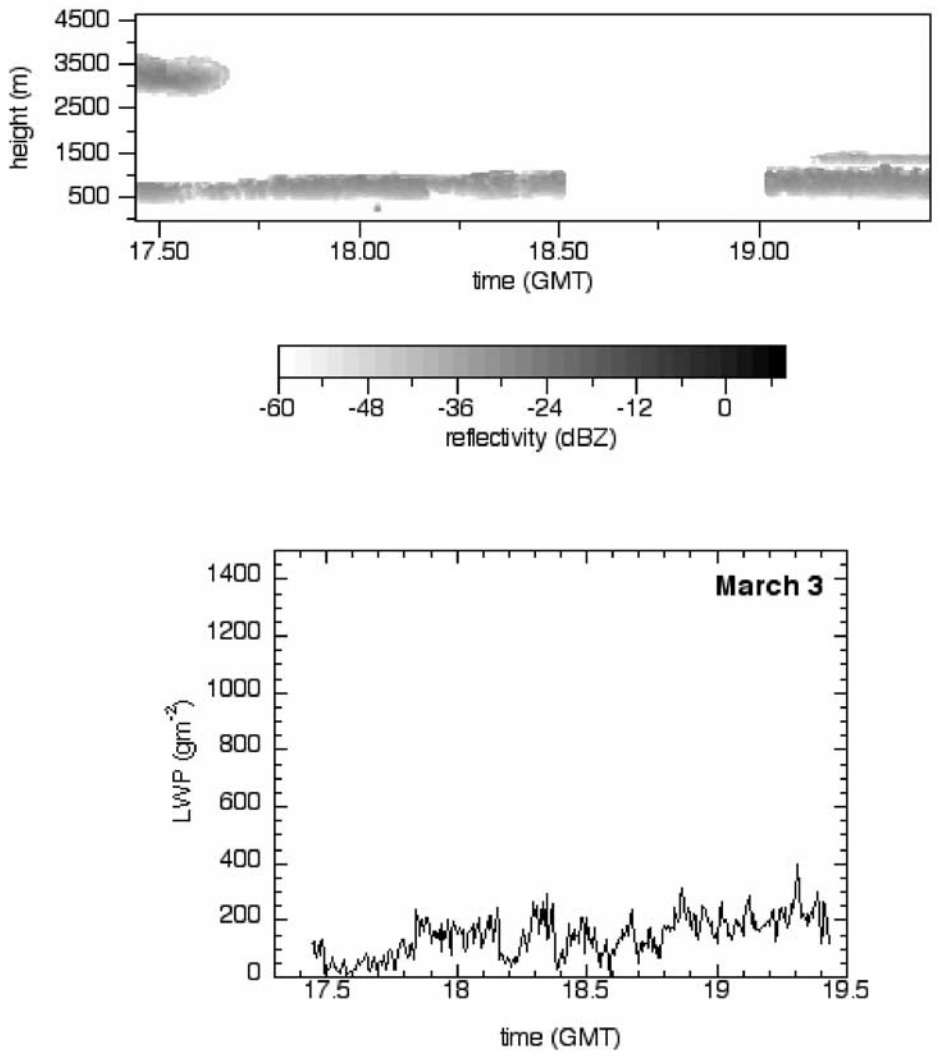

Figure 1. 2-D cloud reflectivity from the MMCR (top) and LWP at the CART site from the MWR (bottom) for the time period when the Twin Otter was flying above the cloud deck. (a) 3 March, (b) 21 March, and (c) 29 March. The gap in the 3 March MMCR display is not due to the absence of clouds but due to the lack of data in the reflectivity product.

repeatedly over the Central Facility at an altitude of ~7 km (when observing clouds) describing a daisy pattern and measuring broadband and spectral shortwave fluxes, while an identical set of instruments was deployed on the ground. The ARESE II ground measurements were complemented by the routine continuous measurements of the ARM operational instrument network. The purpose of ARESE II was to extend the measurements of cloudy sky solar absorption of ARESE I, while addressing the unresolved issues by (1) significantly increasing the number of thick cloud cases, (2) providing more spectral measurements, and (3) where possible, including two or more independent instruments to measure the same component of the solar flux [*Ellingson and Tooman*, 1999]. Partial temporal overlap with a Cloud Intensive Observation Periods (IOP) was intended for good cloud characterization.

[4] This paper analyzes ARESE II measurements for cloudy days only. In addition to comparisons of cloud broadband absorptances from three different sets of instruments (section 3), it investigates sampling and measurement quality issues with the aid of narrowband visible absorptances and discusses interday differences related to cloud morphology (section 4).

2. Data Set and Cloud Absorptance Calculation Method

[5] We analyzed data for three days with stratus clouds: 3, 21, and 29 March 2000. These days were chosen because they were characterized by the ARESE II field participants as the ''best'' from an instrument performance and data quality standpoint. Photographs of the cloud decks from the Twin Otter can be found on the World Wide Web at http://armuav.atmos.colostate.edu/uavw00/uavw00.html for 3 and 29 March. 2-D views of cloud location are provided by the Millimeter Cloud Radar (MMCR) (Figure 1, top panels). Quantitative descriptions of the physical and optical properties of the clouds are obtained from a wide range of surface, airborne, and spaceborne instruments such as surface Microwave Radiometer (MWR), ceilometer, lidar, Scanning

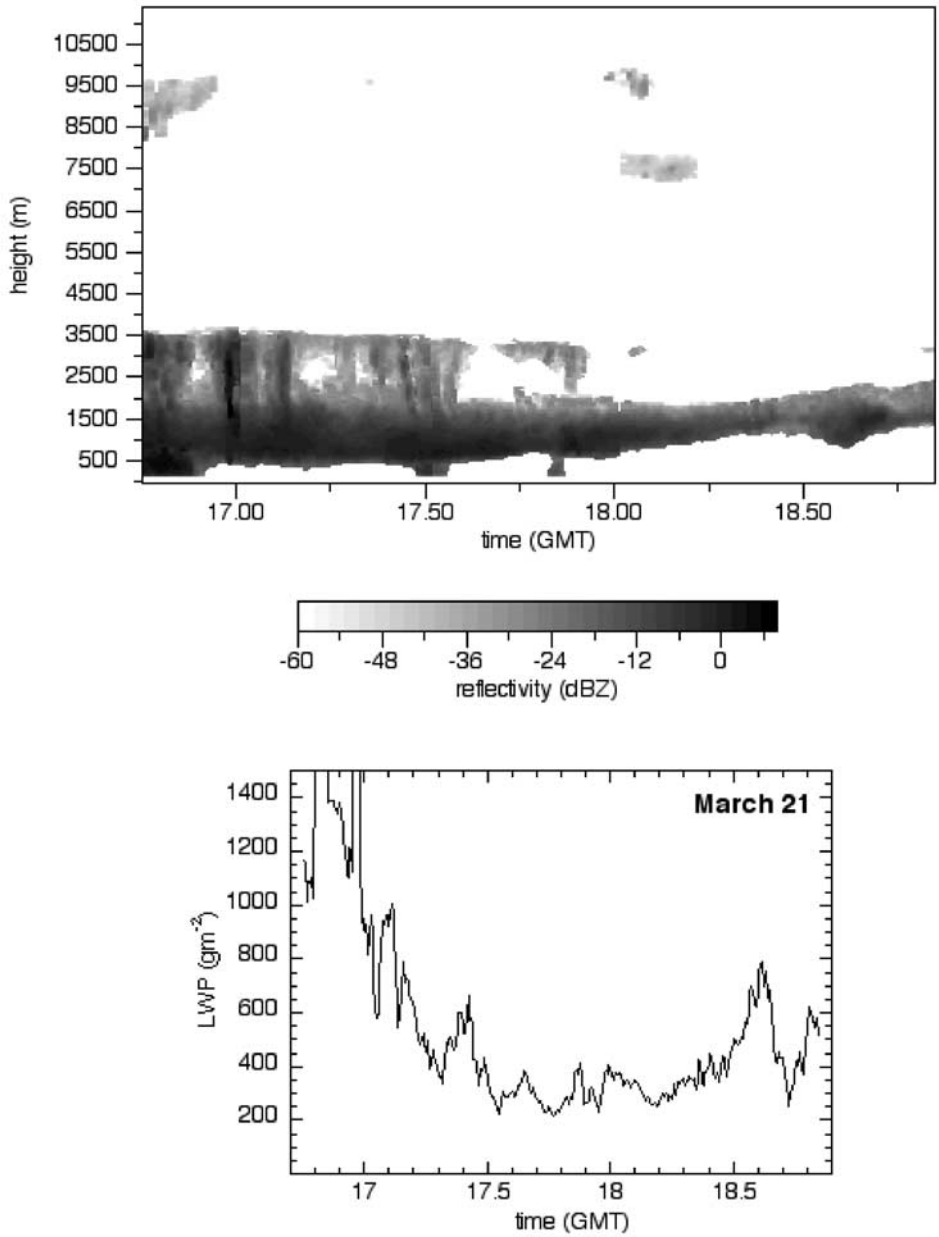

Figure 1. (continued)

Spectral Polarimeter 2 (SSP2) [*Stephens et al.*, 2000], Airborne Cloud Radar (ACR), Forward Scattering Spectrometer Probe (FSSP) (the latter two aboard the Citation aircraft used during the cloud IOP), GOES-8 imager, and Enhanced Thematic Mapper+ (ETM+) aboard Landsat-7, among others. For example, Figure 1 (bottom panels) shows the liquid water path (LWP) time series from the archived ARM data set corresponding to the portion of the Twin Otter flight at ~7 km. Cloud description obtained from these instruments can be used as input to radiative transfer simulations that compare model estimates with the radiometric observations of ARESE II [e.g., *Valero et al.*, 2003] (W. O'Hirok and C. Gautier, Absorption of shortwave radiation in a cloudy atmosphere: Observed and theoretical estimates during the second Atmospheric Radiation Measurement Enhanced Shortwave Experiment (ARESE), submitted to *Journal of Geophysical Research*, 2002, hereinafter referred to as O'Hirok and Gautier, submitted manuscript, 2002; T. P. Ackerman et al., Quantifying the magnitude of anomalous absorption, submitted to *Journal of Geophysical Research*, 2002, hereinafter referred to as Ackerman et al., submitted manuscript, 2002).

[6] In our study, the ARESE II data come from instruments that measure radiative fluxes at both the Twin Otter flight level and on the ground. Specifically we use Twin Otter nadir and zenith pointing TSBR [*Valero et al.*, 1982], FSBR, CM21, CM22 radiometers for broadband, and TDDR [*Valero et al.*, 1989] for spectral measurements, as well as their zenith (upward) pointing counterparts on the ground (when available). We analyze the most recent data releases provided by the instrument PIs to the ARESE II data archive at http://iop.archive.arm.gov/arm-iop/. The full

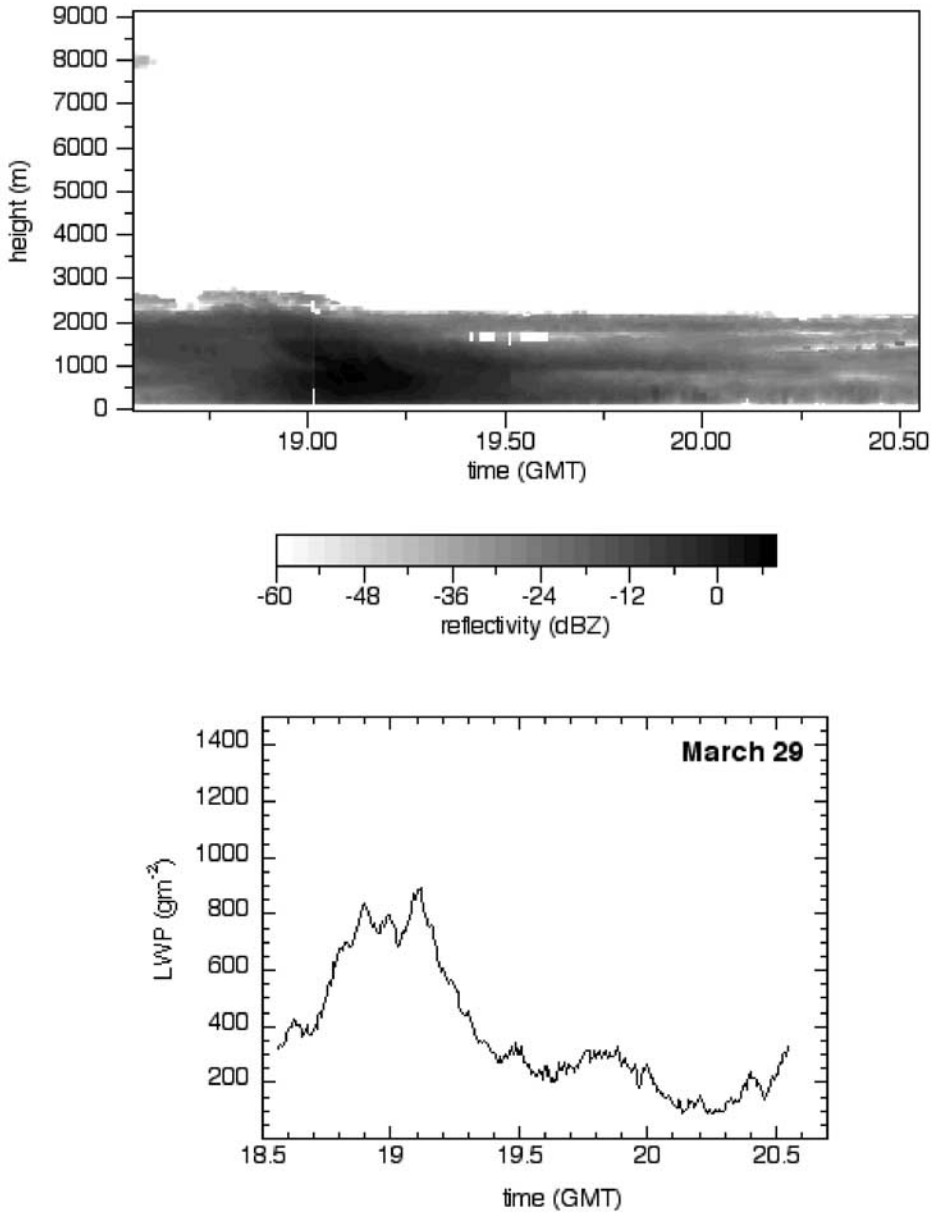

Figure 1. (continued)

names of the radiometers and their spectral range are provided in Table 1. TSBR, FSBR, and TDDR were operated by the Scripps Institution of Oceanography, while CM21 and CM22 were operated by the Meteorological Research Institute of Japan and Sandia National Laboratory, respectively. The calibration of the broadband radiometers against the same standard instruments is discussed by *Michalsky et al.* [2002], while spectral calibration and stability issues are discussed by P. Kiedron et al. (Absolute calibration of ARESE II spectrometers and spectral radiometers, submitted to *Journal of Geophysical Research*, 2002).

[7] Visible or broadband absorption fluxes (F_{abs}) for the ARESE II atmospheric layer between 0 and ~7 km are estimated from

$$F_{abs} = (F^{o}_{dn} - F^{o}_{up}) - (F^{s}_{dn} - F^{s}_{up}) \quad (1a)$$

which can be rewritten as

$$F_{abs} = (F^{o}_{dn} - F^{o}_{up}) - (1 - \alpha)F^{s}_{dn} \quad (1b)$$

The first term in parenthesis is the net solar flux at the Twin Otter level (difference between downwelling, F^{o}_{dn}, and upwelling fluxes, F^{o}_{up}), and the second term is the net flux at the surface (F^{s}_{dn} is the downwelling flux at the surface, F^{s}_{up} the upwelling flux at the surface, and α is the surface albedo). The Twin Otter net flux is measured by aircraft radiometers facing upward and downward, while the surface net flux is measured by ground upward facing (measuring F^{s}_{dn}) and Cloud and Radiation Testbed (CART) tower downward and upward facing Eppley PSPs (Precision Spectral Pyranometers). The latter two provide estimates of α as a flux ratio. The fractional absorptance A is obtained

Table 1. Data From the Following Instruments Were Examined for This Study

Instrument	What it Measures or What can Be Inferred
TSBR, Total Solar Broadband Radiometer	Broadband fluxes 0.2–3.9 μm
FSBR, Fractional Solar Broadband Radiometer	Broadband fluxes 0.68–3.3 μm
TDDR, Total Direct Diffuse Radiometer	Narrowband visible fluxes (7 channels)
CM21, Kipp & Zonen pyranometer	Broadband fluxes 0.3–2.8 μm
CM22, Kipp & Zonen pyranometer	Broadband fluxes 0.2–3.6 μm
MFRSR, Multifilter Rotating Shadowband Radiometer	Narrowband solar fluxes at 6 solar bands below 1 μm
MFR, Multifilter radiometer	Narrowband solar fluxes at the 6 solar MFRSR bands
RSS, Rotating Shadowband Spectrometer	Spectral fluxes, 0.35–1.075 μm
MWR, Microwave Radiometer	Water vapor, cloud liquid water path, from microwave sky radiation at 23.8 and 31.4 GHz
MMCR, Millimeter Cloud Radar	Cloud reflectivity (35 GHz), cloud location

[cf. *Valero et al.*, 2000] from (1b) by simply dividing by F^{o}_{dn}:

$$A = 1 - R - T(1 - \alpha) \tag{2}$$

R and T are the albedo and transmittance for the atmospheric layer between the aircraft flight altitude and the ground. The physical interpretation of (2) is that the total absorption of the Earth–atmosphere system $1 - R$ is the sum of the atmospheric absorption A and the surface absorption $T(1 - \alpha)$.

[8] Time series of A for flight segments when the Twin Otter is above clouds can be obtained by using simultaneous ground and air observations in (1) and (2). The absorbed flux or absorptance time series obtained from the above equations for ARESE II should be characterized as a *pseudoabsorptance* time series since at a particular instant there is in general no well-defined vertical atmospheric column that contains the fields of view of the aircraft and ground instruments and to which the absorption can be attributed to. Such a column can only be defined during the short time periods when the aircraft flies over or near the CART site. These pseudoabsorptances can be considered a generalization of the *apparent* absorptances that are obtained for well-defined atmospheric columns and which comprise the effect of net horizontal flux of photons due to 3-D effects [*Marshak et al.*, 1999]. Thus, in ARESE II there are two reasons why instantaneous fluxes obtained from (1) (or fractional fluxes obtained from (2)) can be nonzero even for a perfectly conservative atmosphere: (1) horizontal fluxes for collocated (Twin Otter above CART site) measurements and (2) distinct fields of view for the ground and aircraft radiometers, i.e., instruments observing different clouds at a particular instant. We will refer to the latter effect as the "*sampling* effect" of ARESE II. It should be distinguished from the more general sampling issue of how representative ARESE II measurements are of cloudy shortwave absorption of a particular latitude zone and season. One of the reasons the planners of the experiment chose the "daisy" flight pattern, in which the aircraft remains within a limited domain and flies repeatedly over the CART site, was to minimize the sampling biases of noncollocated measurements. The goal was to increase the probability that clouds similar to those observed from the ground are viewed from above. In the following we will show that despite the limited nature of the instantaneous values of A obtained from (2), they are linked in a physically meaningful manner to the true atmospheric absorption during ARESE II. Therefore, we will not be using the term "pseudoabsorptance" henceforth.

[9] Finally, we note that in the ensuing analysis fluxes F^{o}_{dn}, F^{o}_{up}, and F^{s}_{dn} used in (1b) are measured always by three identical instruments, in other words, measurements from different types of instruments are never combined to calculate absorptance. The surface albedo α in (1b) and (2) is considered an independent quantity and as explained below is obtained from CART 10 m tower measurements that are part of the regular ARM data set. Thus, from three different triplets of broadband instruments, three different time series of broadband absorptance are obtained, for three days in March 2000.

3. Absorptance Estimates

3.1. Broadband Absorption

[10] Figure 2 summarizes the grand average (average over the entire flight) values of the fractional flux terms of (2) for the three sets of broadband instruments. Broadband surface albedo comes from 10 m tower flux measurements by upward and downward facing Eppley PSP pyranometers. The most nearly simultaneous available

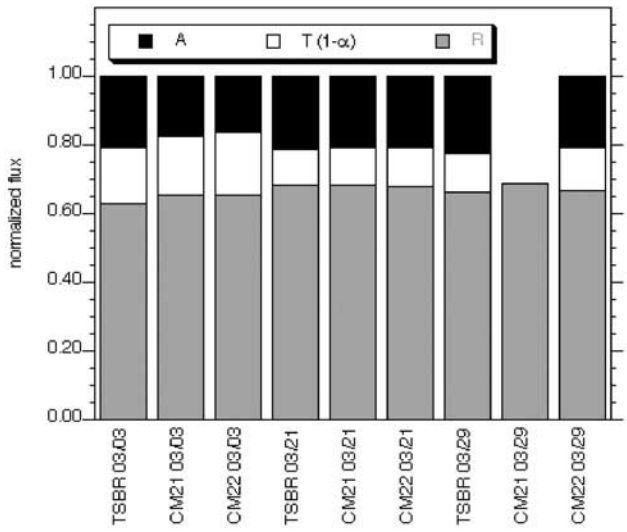

Figure 2. Above-cloud flight grand averages of all components of the fractional flux energy budget (2) for the atmospheric layer defined by the surface and the Twin Otter aircraft. Three days and three sets of instruments are shown. Only albedo at the Twin Otter level (~7 km) is shown for CM21 on 29 March, because no CM21 ground data were available.

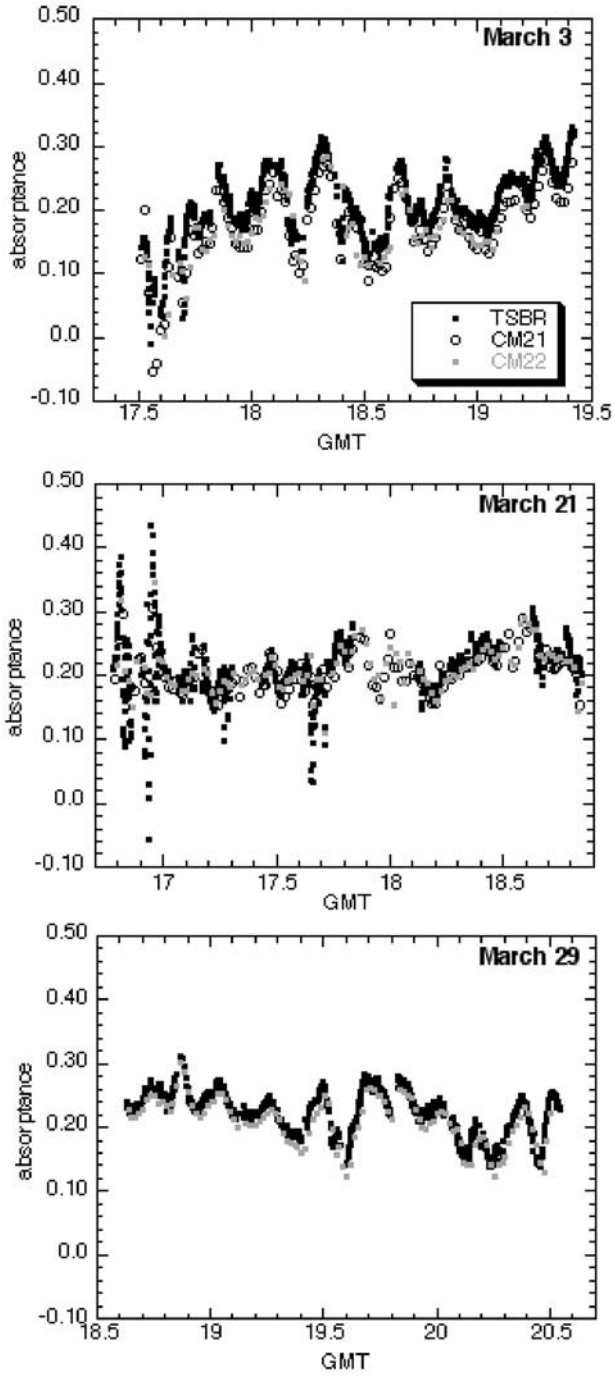

Figure 3. Time series of broadband absorptance for the atmospheric layer defined by the surface and the aircraft flying above clouds. The same three days and three sets of instruments as in Figure 2 are included in the plots. No CM21 absorptance was calculated for 29 March, because of the unavailability of ground data.

value is used, although there is not much variability with time; surface albedo values range from 0.17 to 0.19 for 3 and 21 March and from 0.15 to 0.17 for 29 March. We must note here that surface albedo measurements were also taken by the Twin Otter, following the above-cloud portion of the flights, by flying at low altitudes above the surface (~400–500 m) and below the cloud decks. These surface albedos are used by other investigators [e.g., *Valero et al.*, 2003] (Ackerman et al., submitted manuscript, 2002) in their estimates of absorption. This approach is also sensible because (1) the surface albedo is sampled for an area more representative of that covered by the aircraft during the above-cloud part of the flight and (2) changes in the solar elevation that may have taken place between flights above and below cloud should not have a great influence on surface albedo for cloudy skies since most of the radiation reaching the surface is diffuse. Our rationale for using the tower values of α is that the product $T(1 - \alpha)$ of (2) is calculated in a self-consistent manner from stable platform measurements that are collocated at the ground. An extensive discussion on pros and cons of surface albedo measurements from the Twin Otter and the CART tower, their differences on clear and cloudy days, and their impact on estimates of column absorption is given by Ackerman et al. (submitted manuscript, 2002).

[11] No CM21 ground measurements were taken on 29 March, so for that instrument only the albedo R is shown. Figure 1 shows that clouds were generally thinner on 3 March and thickest on 21 March. This is consistent with the lower values of R for 3 March compared to 21 March in Figure 2, despite the higher solar zenith angle. Figure 2 also shows that TSBR values of A are quite similar on all three days (~0.21–0.22) and that there is quite good agreement among all three (two) sets of instruments for 21 March (29 March), but substantial disagreement on 3 March. The fluxes that correspond to the TSBR absorptances of Figure 2 are ~200–230 W m^{-2}. We have estimated that a 50% error in the surface albedo has a maximum absorption impact of 17 W m^{-2} (~0.02 in terms of fractional absorptance) on 3 March when T was the largest. To put this in perspective, we note that *Michalsky et al.* [2002] estimated the total effect of instrument uncertainty on column absorption for ARESE II to be 20 W m^{-2} at the 95% confidence level.

[12] Figure 3 shows the time series of apparent broadband absorptance for the three days and the three sets of instruments, as derived from (2). Whenever the three absorptances differ substantially, the source of the discrepancy can be traced back to the Twin Otter fluxes. Figure 4 shows the net Twin Otter fluxes. The lower absorptance values of CM21 and CM22 on 3 March, compared to TSBR, are the combined result of lower downward and higher upward flux for the first two instruments (not shown). Surface net fluxes (and hence downward fluxes, since the same surface albedo was used) are in good agreement, as seen in Figure 5.

[13] Other papers [*Valero et al.*, 2003] (O'Hirok and Gautier, submitted manuscript, 2002; Ackerman et al., submitted manuscript, 2002) discuss how the measured absorptances of ARESE II compare with radiative transfer simulations for both clear and cloudy skies. As discussed therein, it appears that the gap between observed and modeled cloud absorption has narrowed compared to ARESE I.

3.2. Absorption at Visible Wavelengths

[14] Estimates of absorption at visible wavelengths can be used to assess the quality of broadband absorptances and correct for sampling effects [*Ackerman and Cox*, 1980;

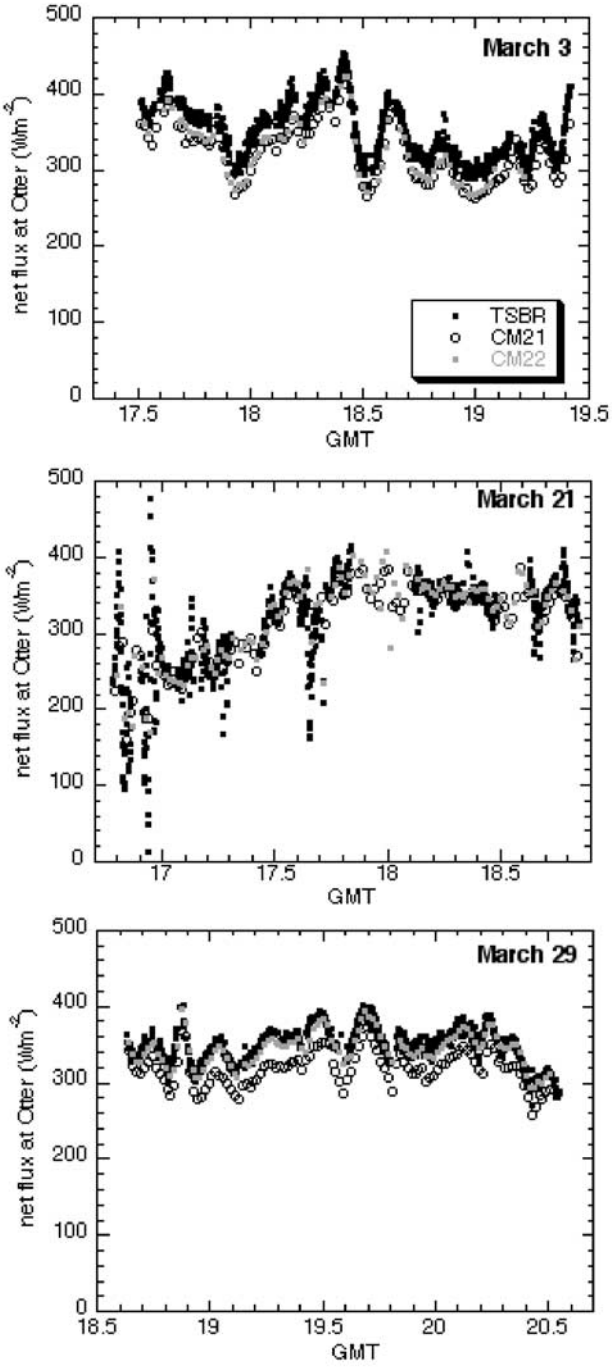

Figure 4. Time series of net broadband flux (down minus up) at the Twin Otter level (∼7 km) for the same three days and three sets of instruments as in Figures 2 and 3.

Valero et al., 1997a; *Marshak et al.*, 1997, 1999; *Cess et al.*, 1999]. One of the main concerns in ARESE-type derivations of cloud absorption is whether averaging fluxes over the entire length of the time series is sufficient to eliminate horizontal flux and sampling ''contamination'' and yield reliable values of *true* absorptance. These issues are discussed more thoroughly in section 4. Here, we simply examine whether the ∼2 hour averages of apparent 500 nm absorptance are consistent with what is expected from conservative cloud droplet scattering and the absence of significant gaseous absorption at this wavelength for the surface-Twin Otter atmospheric layer.

[15] Figure 6 shows the time series of 500 nm apparent absorptance A_{500} for the three March days, estimated from the Twin Otter and ground TDDR instruments using (1) and (2). For surface spectral albedo, we use again the closest

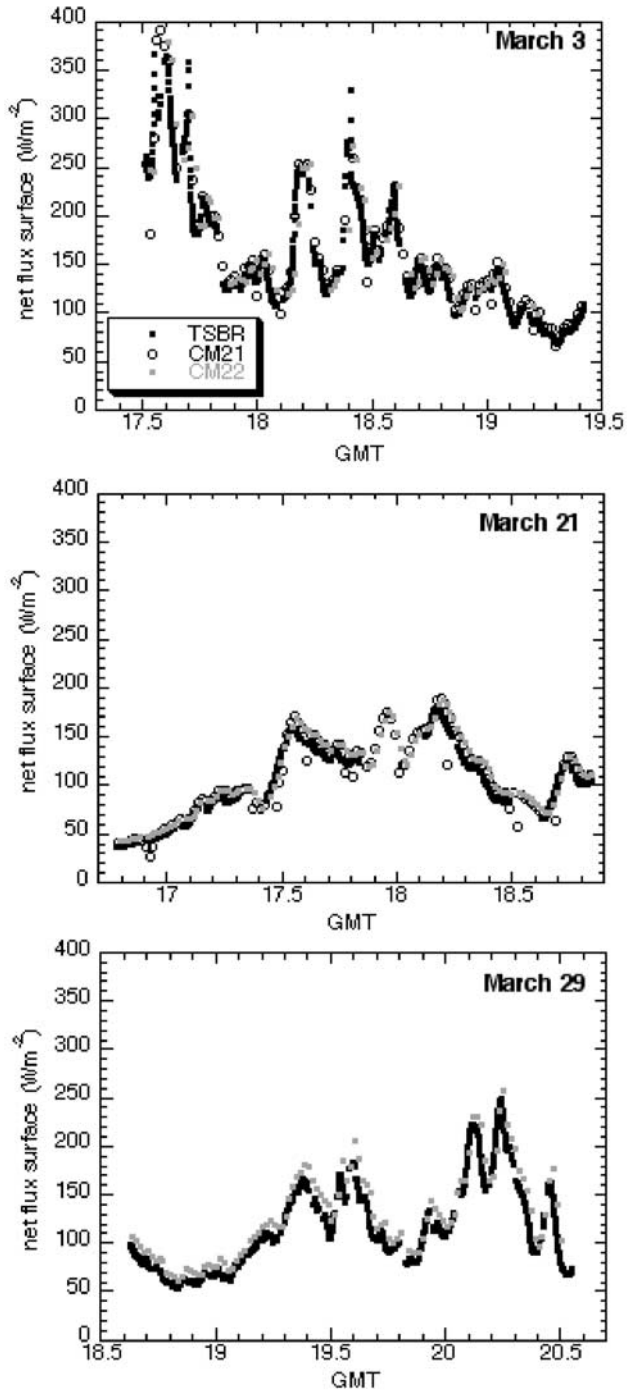

Figure 5. Time series of net downward fluxes $(1 - \alpha)F^{S}_{dn}$ for three ARESE II days and three sets of instruments corresponding to the above cloud flight segment. There were no CM21 ground measurements available on 29 March.

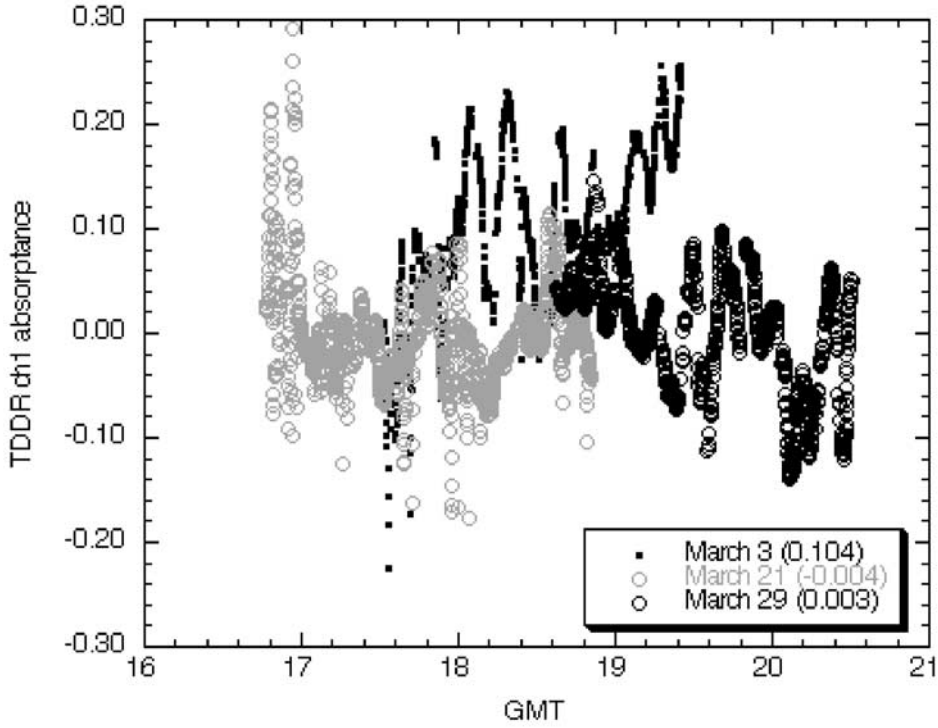

Figure 6. Time series of TDDR channel 1 (500 nm) absorptance for the three cloudy ARESE II days of our study. The grand averages of the time series are shown in parenthesis in the legend.

value in time from the ARM data archive (values range from 0.07 to 0.08 for 3 and 21 March and from 0.04 to 0.06 for 29 March). This albedo applies for the vicinity of the CART tower and is estimated as the ratio (at 10 m) of MFR upwelling and MFRSR (Table 1) downwelling flux. 3 March is quite different from the other two days with large (0.104) positive grand average absorptance $\langle A_{500} \rangle$, while 21 March (-0.004) and 29 March (0.003) estimates are virtually indistinguishable from zero and therefore closer to anticipated values. For 3 March, the average of the 475 nm and 525 nm fluxes (channels 3 and 4 of TDDR) produced virtually identical aircraft net and surface downward fluxes as the 500 nm channel, in agreement to instrument design specifications (Valero, personal communication, 2002). Absorption at TDDR channel 7 (675 nm) was also close to 500 nm values (not shown). Thus, other TDDR channels do not help explain the distinct behavior at 500 nm on 3 March. We believe that the surface fluxes are reliable for that day since TDDR surface measurements agree well with other surface instruments such as MFRSR and RSS. It is noteworthy that there are several flight legs (see Figure 12 later) for which the average 500 nm absorptance exceeds 0.10. Insufficient sampling under broken cloud conditions (see also section 4.2 below) of fluxes which are already very sensitive to errors due to the small amounts of energies involved, may be the reason behind these high values. We must stress that ''back of the envelope'' radiative transfer calculations indicate that it is possible to obtain 500 nm absorptances of $\sim$0.1 for aerosols of $\sim$0.9 single scattering albedo and optical depth $\sim$0.4–0.5 (at 500 nm) coexisting with clouds, but such high aerosol loadings were not observed at the SGP site during the clear days of March 2000 (cf. http://aeronet.gsfc.nasa.gov/). Moreover, if a high concentration of absorbing aerosols was present there would be a perceptible effect on the broadband absorptances as well, which is not the case (Figure 2). The ARESE II 500 nm absorptance results are in sharp contrast with the notably constant 500 nm average absorptances of $\sim$0.05 in ARESE I, where all the absorption was attributed to aerosols [*Cess et al.*, 1999]. Assuming an atmosphere with very low or no aerosol loading, the near zero grand averages of 21 and 29 March are quite realistic.

[16] Finally, one can calculate the broadband visible absorptance from the net flux difference of ground and Twin Otter TSBR–FSBR differences. The grand average values for cloudy conditions are 0.04 for 21 March and 0.03 for 29 March. These are lower than in ARESE I [*O'Hirok et al.*, 2000; *Valero et al.*, 2000] where the atmospheric column was larger, but we consider them reasonable values for the atmospheric layer between the aircraft and the ground. They agree quite well with the modeled values of O'Hirok and Gautier (submitted manuscript, 2002). Note, however, that the additional flux difference operations that are required in making these estimates compared to 500 nm make them more prone to error. Other papers (O'Hirok and Gautier, submitted manuscript, 2002) examine in more detail the quality of broadband visible absorptances and how they compare to simulated values.

4. Sampling Issues

4.1. Correlations With LWP

[17] Given the experimental design of ARESE II, an important question is whether the fluxes measured at the

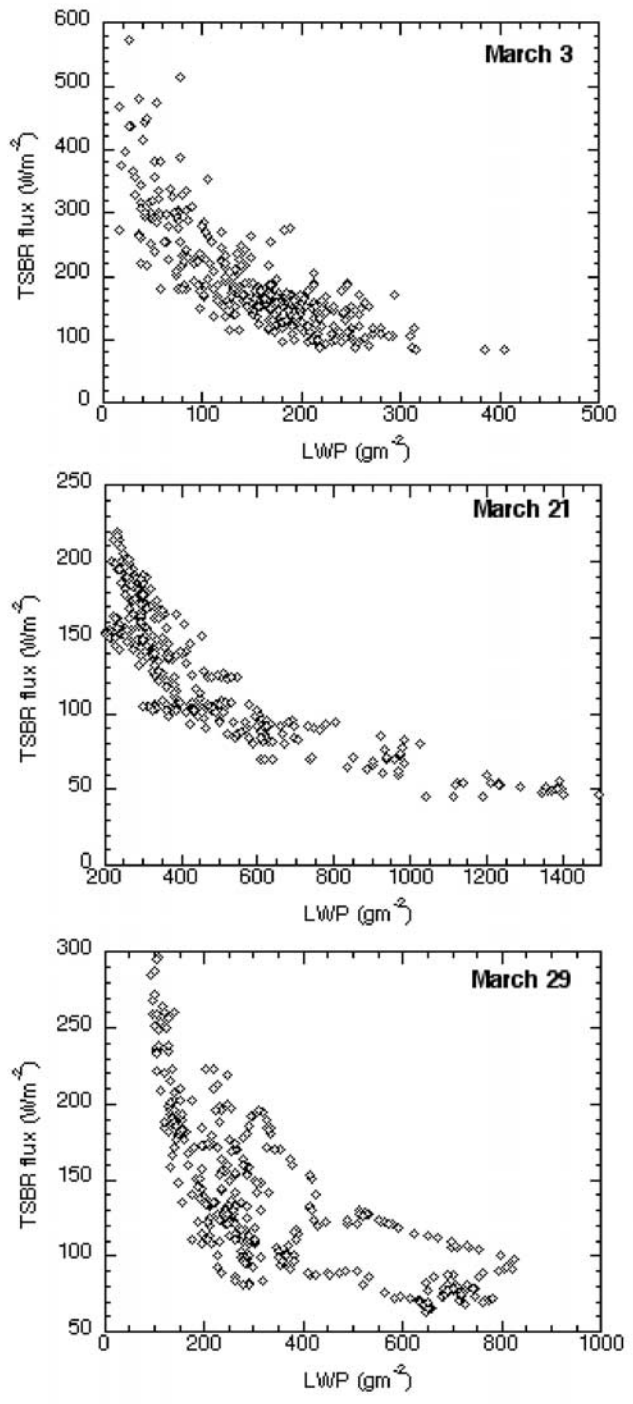

Figure 7. Broadband surface TSBR flux versus LWP from the MWR for the three March days, when TSBR fluxes are averaged at the temporal resolution (20 s) of the MWR data.

ground result from attenuation by the same (in a statistical sense) clouds that largely determine the Twin Otter reflected fluxes as the aircraft flies along the daisy pattern. There is more confidence that statistically similar conditions prevail when the clouds are extensive and homogeneous. The clouds that primarily control the surface fluxes are described quite well (in terms of liquid water path) by the MWR because of its close proximity at the CART site to the surface flux radiometers. This can be seen in scatterplots of downward flux (either broadband or narrowband) versus LWP (Figure 7). On the other hand, upward fluxes or atmospheric column albedos generally do not correlate well with the MWR LWP (Figure 8a) because of the lack of

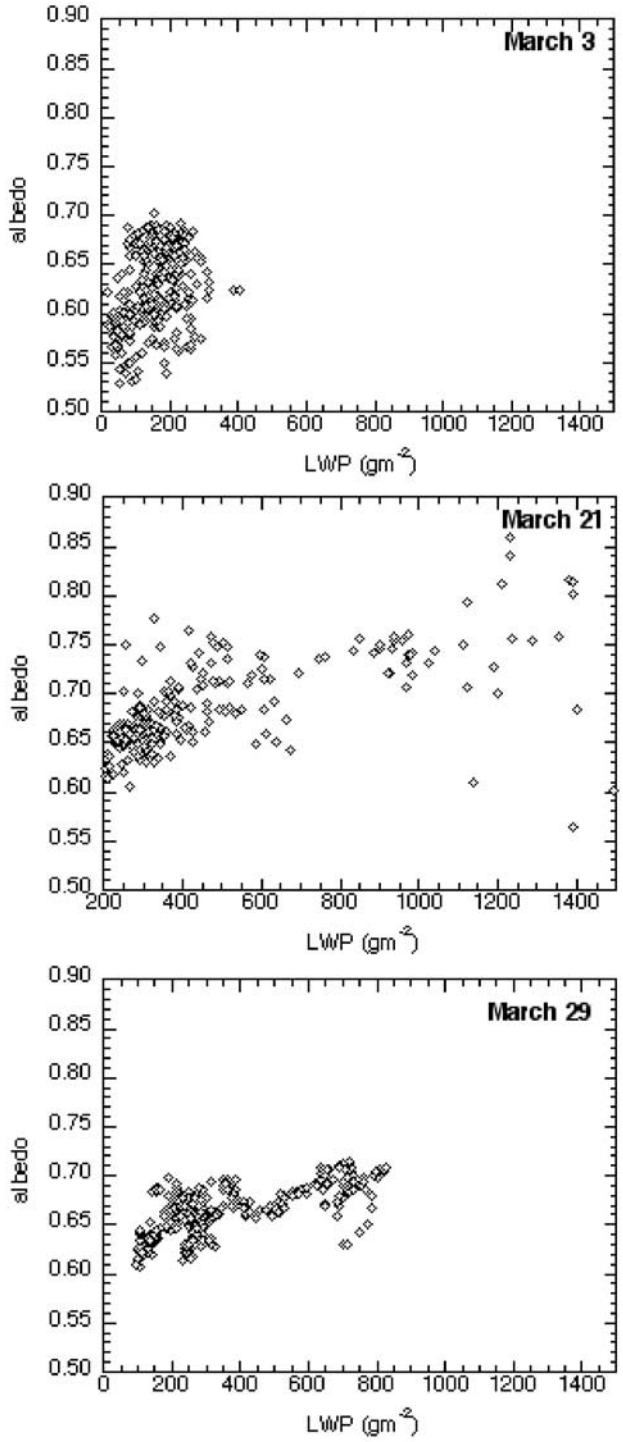

Figure 8. Broadband Twin Otter TSBR albedo versus LWP from the MWR for the three March days, when TSBR fluxes are averaged at the temporal resolution (20 s) of the MWR data.

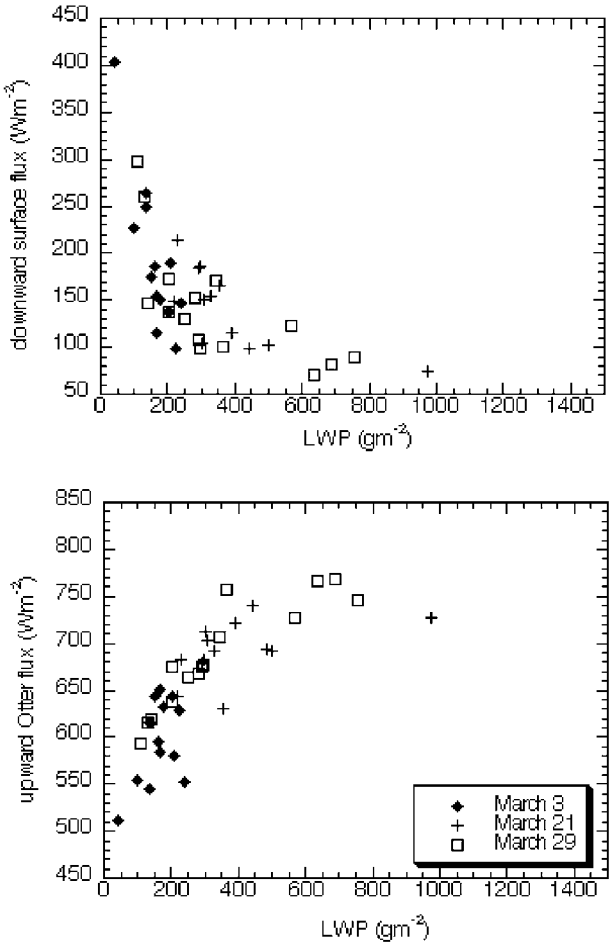

Figure 9. Broadband TSBR downward fluxes (top) and upward fluxes (bottom) versus LWP from MWR for data points corresponding to aircraft overpass over the CART site (aircraft is within a 0.02° square centered at CART).

collocation. An additional factor that worsens the correlation with upward fluxes is the larger cloud area viewed by the Twin Otter pyranometers which sample at heights 3–5 km above cloud top. This effect is more pronounced on 3 March when the Twin Otter is farthest away from cloud top. Note that the surface downward flux correlation with LWP and the absence of significant correlation with Twin Otter upward (and hence net) flux leads to *deceptive* LWP correlation with absorptance! Such correlation does not indicate any physical processes, but is rather an artifact of spatial collocation for the surface instruments and the sampling design of the experiment.

[18] Interestingly, on 21 and 29 March (Figures 8b and 8c), there is some positive correlation even with the upward Otter flux, suggesting that either the Twin Otter sampled the clouds in a time sequence similar to the MWR (21 March, Figure 1b) or that clouds were quite homogeneous (29 March, Figure 1c). Unsurprisingly, when the Otter passes over the CART site, both Otter upward and surface downward fluxes are well correlated with LWP (Figure 9). Some investigators (e.g., O'Hirok and Gautier, submitted manuscript, 2002; S. Asano et al., Solar radiation budget from the MRI radiometers for the clear and cloudy air columns in the ARESE II, submitted to *Journal of Geophysical Research*, 2002) use only these collocated points in their analysis. Interestingly, the broadband and visible absorptance mean values for the collocated measurements are very close to the grand averages of the entire time series quoted earlier. Specifically, the broadband mean values from collocated measurements for TSBR are 0.204, 0.200, and 0.219 for 3, 21, and 29 March, respectively; the 500 nm mean values are 0.084, −0.016, and −0.003, i.e., 500 nm absorptance values for 3 March remain much higher than expected (and the modeled broadband visible absorptances of O'Hirok and Gautier (submitted manuscript, 2002)), while 21 and 29 March are zero within TDDR absorption uncertainties (Valero, personal communication, 2002). The mean values of LWP for aircraft overpasses over CART are 162, 396, and 351 g m^{-2}, thus there is no LWP–broadband absorptance correlation as was found by *Zender et al.* [1997] for ARESE I.

4.2. Cumulative Averages

[19] Another approach for investigating possible sampling problems is to examine cumulative averages, à la *Valero et al.* [1997a, 2000]. In Figure 10, we plot the standard deviation of five cumulative averages of TDDR 500 nm apparent absorptances as a function of the fraction of the total number of points in each day's time series. The five cumulative averages were obtained by arranging the data of the time series in five different ways: in the original order the data was collected, with the first 25% of the data moved to the end of the time series, with the first 50% moved to the end, with the first 75% moved to the end and, finally, backwards. Figure 10 shows how closely the grand average is approached when only a fraction of the points is averaged. Better sampling is implied for the curve that remains the closest to the abscissa and asymptotically approaches zero the fastest. Based on these criteria, 21 and 29 March seem to be clearly superior to 3 March, and 29 March has an apparent slight edge over 21 March. The good quality of the 29 March sampling and the internally consistent nature of the measurements for that day will be

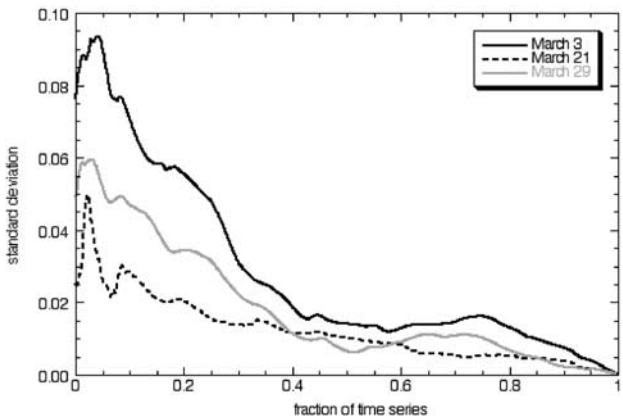

Figure 10. Standard deviation of the five different cumulative averages described in the text as a function of the fraction of the total time series length (total number of points) for the three days analyzed in this paper.

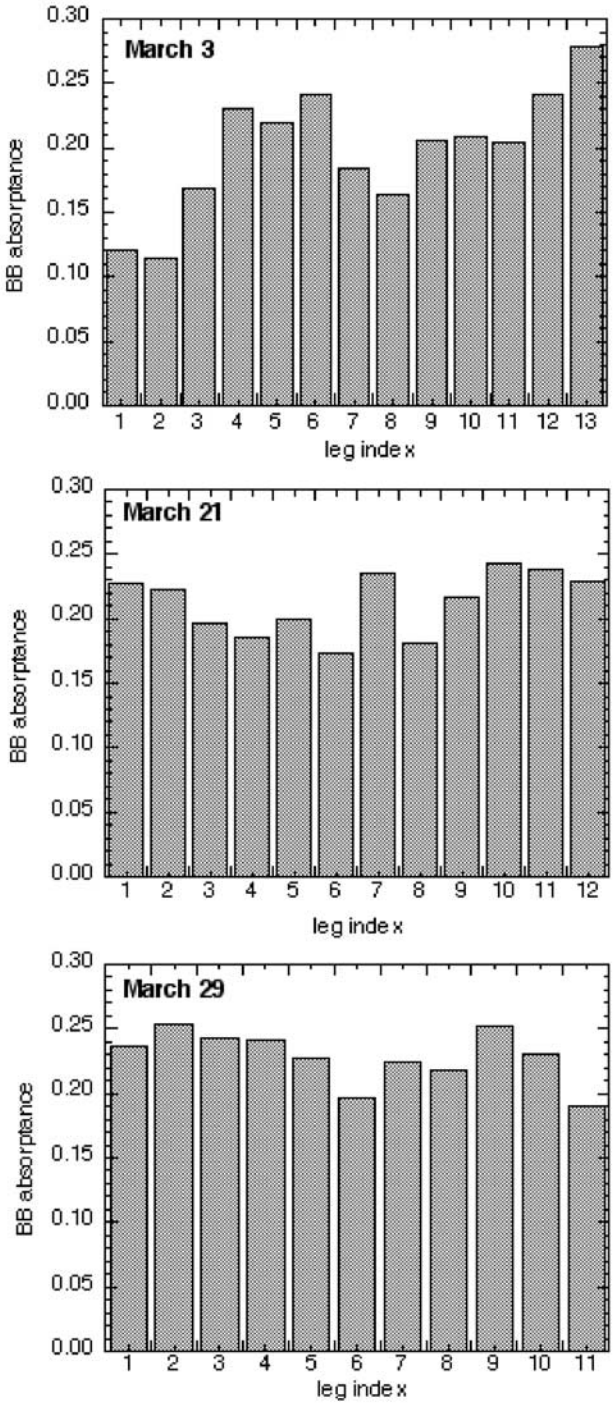

Figure 11. Broadband apparent absorptance per flight leg for the three ARESE II days analyzed.

further supported with more results in the following subsections.

4.3. Analysis by Flight Leg

[20] Here we examine variability among flight legs (flight segments between aircraft turns) and whether averaging over a flight leg is long enough to significantly reduce horizontal flux and sampling effects. Typical flight legs last ~5–8 min, a time period during which the Twin Otter covers distances of a few tens of kilometers. Figure 11 shows the mean TSBR broadband absorptances per flight leg for all three days. 21 and 29 March have a much tighter range of values, suggesting smaller sampling effects than 3 March, for which the first and last leg yielded absorptances that differ by a factor greater than 2. Figure 12 is the 500 nm

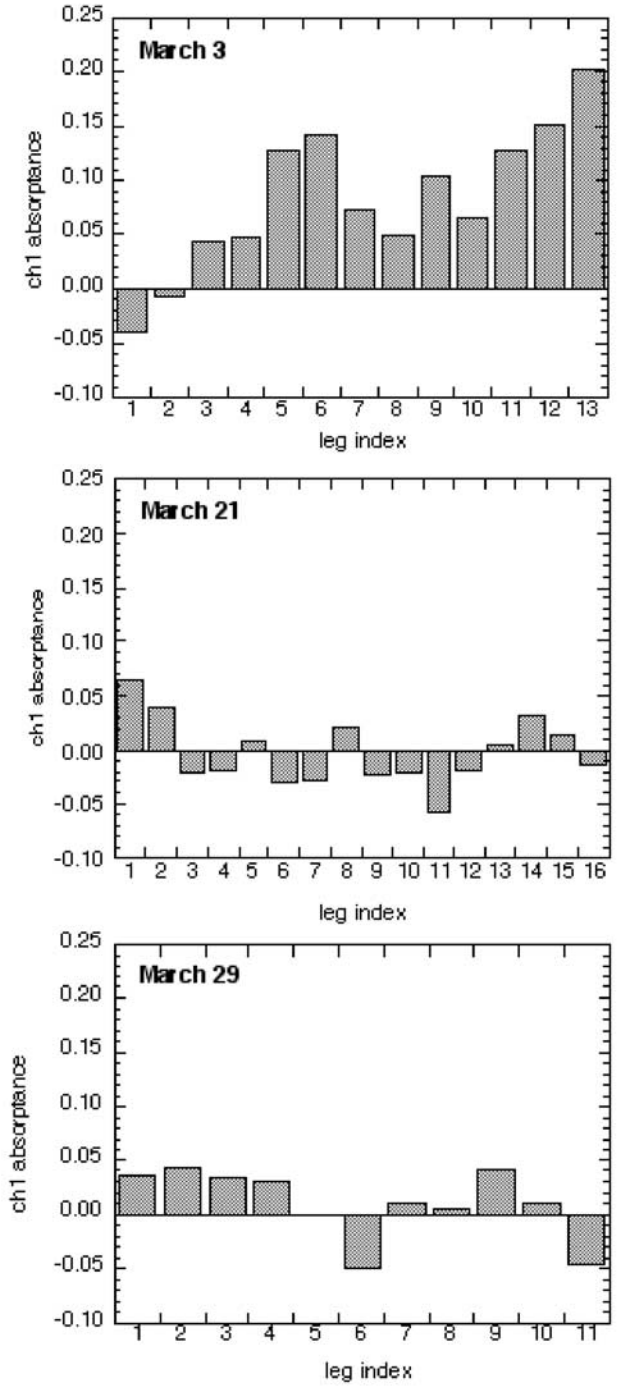

Figure 12. As in Figure 11, but for apparent 500 nm absorptance. For 21 March, the number of legs is different than that of Figure 11 due to the availability of TDDR measurements at time instants where TSBR data where not available.

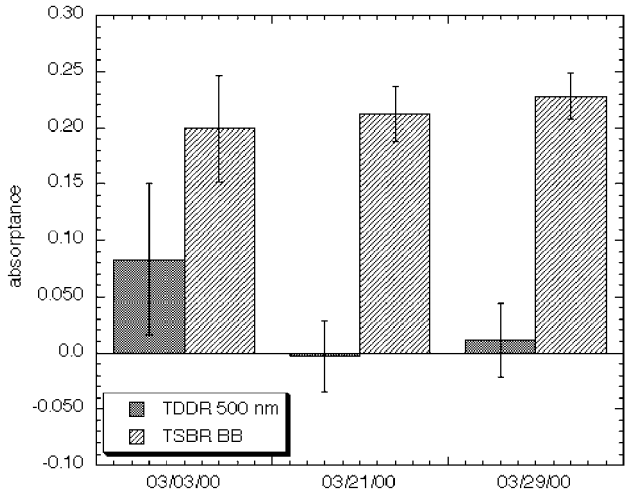

Figure 13. Mean and standard deviation (depicted as error bars) of the data presented in Figures 11 and 12.

TDDR counterpart. On 3 March, flight leg absorptances at 500 nm often acquire high values that do not conform with our knowledge of radiative transfer at that wavelength. This suggests that at the flight leg equivalent spatial scale, clouds observed from the aircraft and the ground may be statistically dissimilar and/or averaging is not sufficient to eliminate horizontal fluxes [*Titov*, 1998; *Marshak et al.*, 1999]. For the other two days, values remain in general within ±0.05, which, considering 500 nm absorption estimate uncertainties, indicates much smaller sampling effects. Figure 13 provides the standard deviation of the flight leg averages as error bars superimposed on the column bars depicting the means of the flight leg averages. The latter are very close to the means of Figures 2 and 6, the small differences being due to the omission of data corresponding to flight legs of very short duration. The 3 March standard deviations are the largest, as expected.

4.4. Conditional Sampling

[21] Conditional sampling is a powerful technique for obtaining reliable absorption estimates without horizontal averaging [*Marshak et al.*, 1999], thus increasing the number of absorption data obtained from a single experiment. One applies conditional sampling to the problem of absorption estimation by first choosing as the *condition* that narrowband spectral absorption values are sufficiently close to their true value, assumed to be known. Broadband values are then selected (i.e., *sampled*) at those instants that lie within the time intervals during which the narrowband measurements satisfy the above condition. For these time instants, the horizontal flux [*Titov*, 1998] is presumed to be small for both narrowband visible and broadband measurements. The narrowband interval is usually at wavelengths where cloud scattering is believed to be conservative, i.e., true absorption A_v^{true}, if any, is horizontally invariant and only due to gases and aerosols. Ideally, the value of A_v^{true} can be theoretically predicted given the appropriate input from independent measurements. Failing that, it must be assumed that the value of true absorption can be obtained from the grand average of the apparent absorptance time series for this narrowband spectral interval, i.e., $A_v^{true} = \langle A_v \rangle$. Narrowband spectral intervals around 500 nm have been used in the past [*Marshak et al.*, 1999; *Cess et al.*, 1999] because the radiative transfer physics in this band is presumed to be well understood. The relevant question then is: can conditional sampling, developed for collocated measurements, such as those during the ARESE I two-aircraft experiment, be applied to the noncollocated ARESE II measurements?

[22] As discussed earlier, for ARESE II, the instantaneous broadband and 500 nm absorptances estimated by (2), and associated horizontal fluxes [*Titov*, 1998] are in general ill-defined because statistically different portions of the cloud field may be viewed at a particular instant from above and below. In other words, in the case of a single-aircraft experiment an estimate $A_{500}(t)$ at time instant t that satisfies

$$\langle A_{500} \rangle - \varepsilon \le A_{500}(t) \le \langle A_{500} \rangle + \varepsilon \qquad (3)$$

where ε is small enough, has lost its special physical meaning as an estimate that is minimally affected by horizontal fluxes. This distinction is reserved only for the few measurements of the well-defined atmospheric columns formed by the aircraft and ground instruments during the short periods of overpass over the CART site.

[23] In spite of the above, we will make the *assumption* that apparent broadband absorptance estimates at time instants t, $A_{BB}(t)$, for which the corresponding 500 nm apparent absorptance $A_{500}(t)$ satisfies (3) are good approximations of the "true" broadband absorptance, even for a single-aircraft experiment such as ARESE II. Our assumption can be justified only if the following two conditions are met: (1) The time series of A_{500} and the grand average $\langle A_{500} \rangle$ are consistent with our understanding of radiative processes at 500 nm. (2) A_{500} and A_{BB} estimates from (2) are well correlated. Figures 15 and 16 that follow confirm that condition (2) is true for ARESE II.

[24] The rationale behind our assumption (subject to the above two conditions) is the following: Assuming for simplicity that $\langle A_{500} \rangle$ and α_{500} are zero and the cloud particle size is constant, all 500 nm measurements that satisfy $R_{500} + T_{500} = 1$ (R_{500}, T_{500} are the albedo and transmittance of the aircraft-surface atmospheric layer at 500 nm) correspond to a unique visible optical depth. Since our second condition, namely that broadband and 500 nm measurements are correlated is met (cf. Figures 15 and 16), we assume that the simultaneous broadband measurements also correspond to that unique optical depth. That is, the measured apparent broadband absorptance is very close to the true broadband absorptance that a perfect broadband model would give for that optical depth. Hence, one should think of the conditional sampling analysis for ARESE II as a method that seeks consistent pairs of R_{500} and T_{500} and their broadband counterparts and not columns (which are not well-defined) with small horizontal fluxes. The first condition, that there has to be confidence in the 500 nm measurements, is also crucial. Since we do not have such confidence for 3 March (large $\langle A_{500} \rangle$ and unexplained trend with time; see Figures 6 and 12), we do not perform conditional sampling for that day.

[25] Figure 14 shows the broadband absorptance (A_{BB}) histogram of the original time series and the histogram of conditionally sampled values for 21 and 29 March. Note

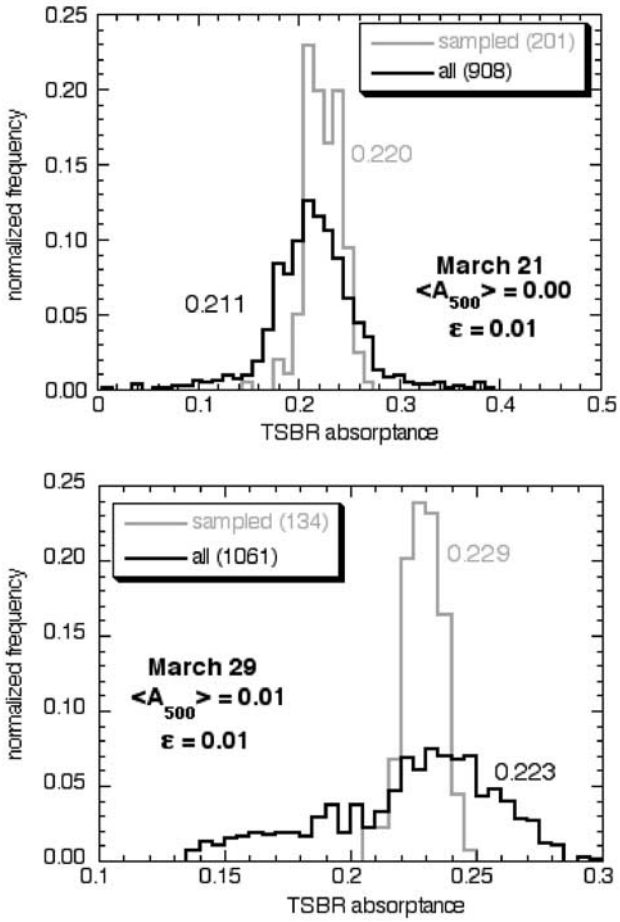

Figure 14. Normalized histograms of broadband absorptance from the original and the conditionally sampled data set for 21 and 29 March. The 500 nm values of "true" absorptance (= grand average) used for the sampling are given in bold and the numbers in the legends given in parentheses are the number of values used to construct the histograms. Also provided are the grand average of the original histogram and the mean of the sampled points.

that because of lack of collocation, the histogram of the original time series has little physical meaning. To create the conditionally sampled histograms, we have selected $\langle A_{500} \rangle = 0$ for 21 March and $\langle A_{500} \rangle = 0.01$ for 29 March based on the results of Figure 13 and $\varepsilon = 0.01$ for both days. The number of conditionally sampled points, as well as the initial number of points are shown in the legend in parentheses. We also compare the mean of the conditionally sampled points with the grand average of the original time series: the former is slightly higher than the latter. Most importantly, however, the histogram of the sampled points is narrower than the original histogram, suggesting that our sampling method does not pick in a random fashion from the original series. The method works better for 29 March, as expected because of better 500 nm and broadband correlations, but still works quite adequately for 21 March, despite the complex cloud morphology.

[26] With the results of Figure 14 in hand, we now have an idea about the range of "true" broadband absorptance values for 21 and 29 March of ARESE II based on the conditional sampling method. This range is approximately 0.18–0.26 for 21 March and 0.21–0.25 for 29 March. High and low extrema outside this range must be treated with caution since there is great chance they are contaminated with 3-D horizontal flux contributions and sampling effects due to noncollocation. The next subsection will present another method to estimate the range of "true" broadband absorptances for ARESE II.

4.5. Absorptance Time Series Correction

[27] In addition to conditional sampling, modifications to the "Ackerman–Cox" [*Ackerman and Cox*, 1980] correction method of 3-D cloud effects, such as those suggested by *Marshak et al.* [1997] and *Cess et al.* [1999], can be applied to the ARESE II broadband absorptance time series. These methods, by design, preserve the grand average of the original absorptance time series, but "correct" the instantaneous values. We implement here the correction described by *Cess et al.* [1999]:

$$A^{c}_{BB}(t) = A_{BB}(t) - c(A_{500}(t) - \langle A_{500} \rangle) \quad (4)$$

$A^{c}_{BB}(t)$, $A_{BB}(t)$ are the broadband absorptances at time t after and before the correction, respectively, $A_{500}(t)$ is the apparent 500 nm absorptance at time t, and $\langle\ \rangle$ stands for time average. c is the slope of the regression fit of A_{BB} versus A_{500} (Figure 15). The premise of the method is that broadband and 500 nm apparent absorptances are correlated (which is confirmed by Figures 15 and 16) and that the correlation exists chiefly because the 3-D radiative and sampling effects operate in a similar way on both broadband and narrowband visible measurements. (4) is an extension of the *Marshak et al.* [1997] correction $A^{c}_{BB}(t) = A_{BB}(t) - cA_{500}(t)$ which applies when $\langle A_{500} \rangle = 0$. *Ackerman and Cox* [1980] originally suggested $A^{c}_{BB}(t) = A_{BB}(t) - A_{500}(t)$, i.e., they assumed that the 500 nm (or any conservative) band has the same horizontal flux as the broadband measurement. However, Figure 15 clearly indicates that $c \neq 1$. We actually find values of c quite close to the 2/3 slope reported by *Marshak et al.* [1997] and *Cess et al.* [1999]. Moreover, we have already seen that for ARESE II 500 nm measurements $\langle A_{500} \rangle$ is not necessarily equal to zero, so the more general equation (4) appears to be the most appropriate. To summarize, (4) as applied to ARESE II data, attempts to remove for each point (instant) the contribution of noncollocation and horizontal flux to the apparent broadband absorptance by using its relationship with the corresponding contribution at 500 nm.

[28] Figure 16 shows the corrected broadband absorptance time series for all three days. The tightening of the time series after the correction has been applied is quite remarkable. Thus, the method seems indeed to be working for noncollocated measurements, because broadband and narrowband visible apparent absorptances are correlated, and is not affected even by the apparent high bias of A_{500} and $\langle A_{500} \rangle$ on 3 March. The corrected absorptances for that day still retain two spikes at ~17.9 and 18.9 GMT. Around these times, the correlation between A_{BB} and A_{500} breaks down (group of points separated from the main cluster in Figure 15a) for unknown reasons, and the correction by (4) is no longer optimal, locally. 21 March is even more complicated. The three different segments of the time series

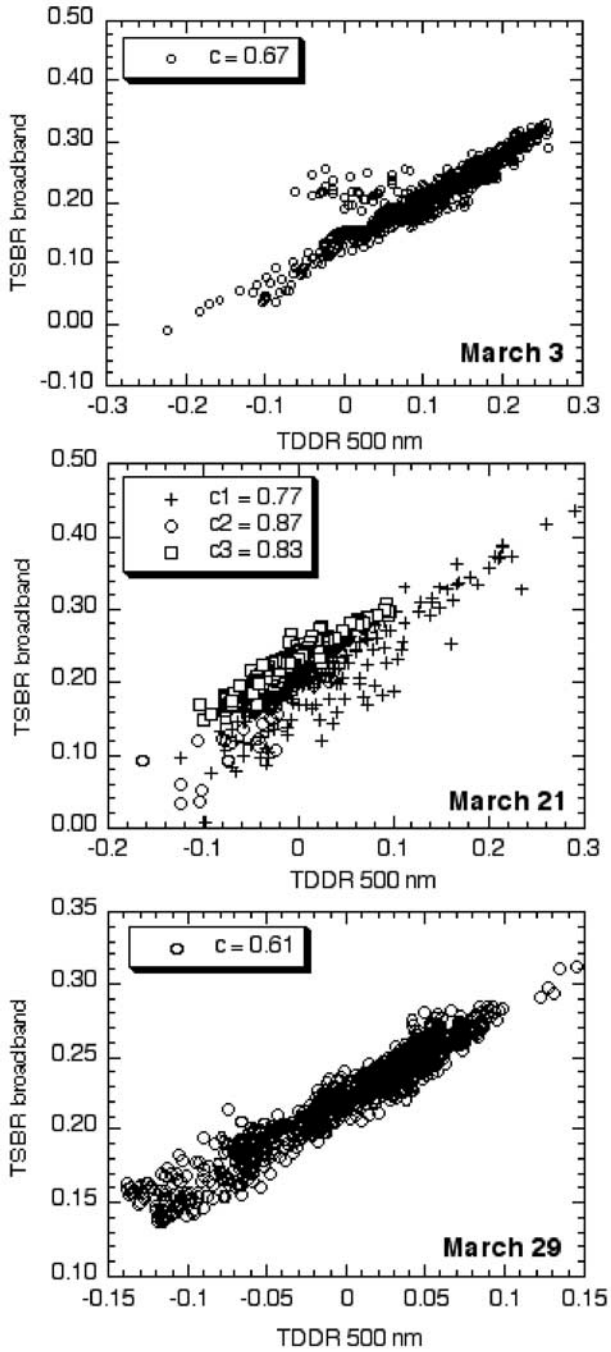

Figure 15. TSBR apparent broadband absorptance versus TDDR 500 nm apparent absorptance for 3 March (top), 21 March (middle), and 29 March (bottom). The *c* values in the legend are slopes of least squares fits. Three separate fits were performed for 21 March, corresponding to the three data segments (separated by wide gaps) shown in Figure 16.

as determined by the two data gaps around 17.4 and 18.0 GMT are also characterized by different cloud types (Figure 1b, top) resulting in different correlations between visible and broadband flux. Fitting a single regression line to the data of Figure 15b would give a meaningless slope, so we perform three individual fits (values of *c* given in the legend of Figure 15b) and apply (4) to each segment separately using its own slope *c*. The correction by (4) is by no means perfect: for example, two dips remain in the A^c_{BB} time series, around 16.85 and 17.7 GMT when cloud structure is complex (upper level cloud, above the Otter, at ~16.85 GMT, unusual cloud top structure and neighboring upper level clouds at 17.7 GMT, according to Figure 1b). Dips in the original absorptance series themselves appear only for TSBR and CM22 (Figure 3). It is disconcerting that clouds above the Otter can affect the values of instantaneous absorptance for the column below. Our explanation is that an overlying small cloud affects the downward Otter flux

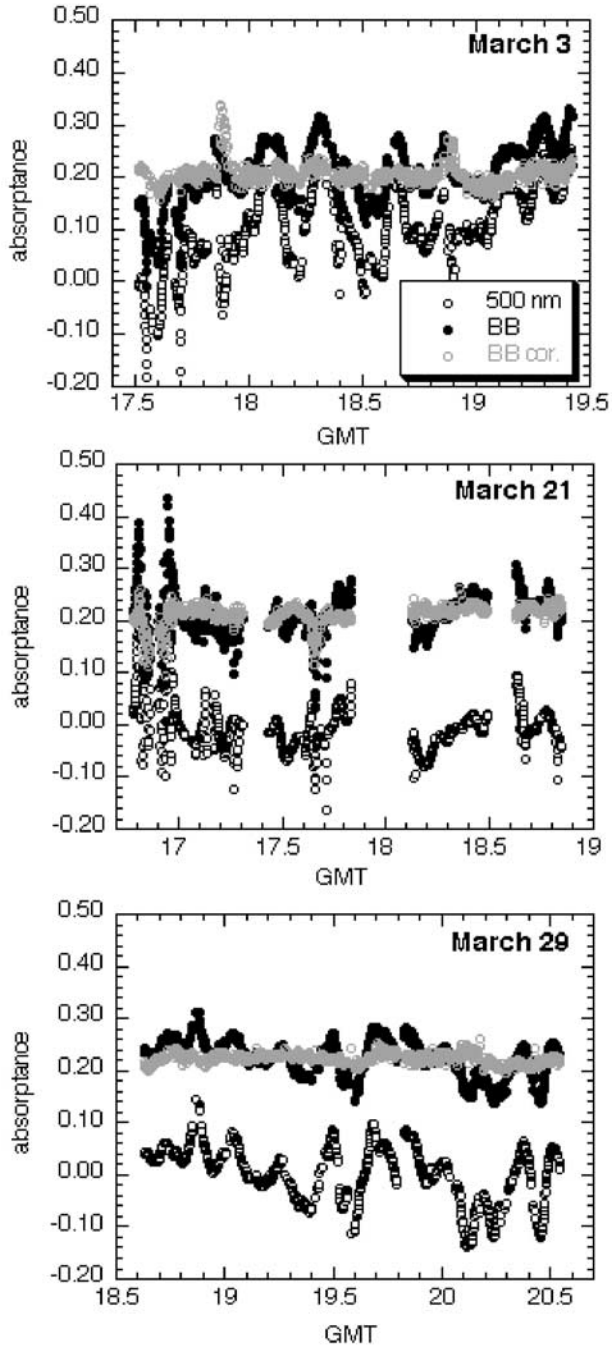

Figure 16. Time series of apparent absorptance for TDDR 500 nm channel, apparent TSBR broadband absorptance (as in Figure 3), and "corrected" TSBR absorptance from (4).

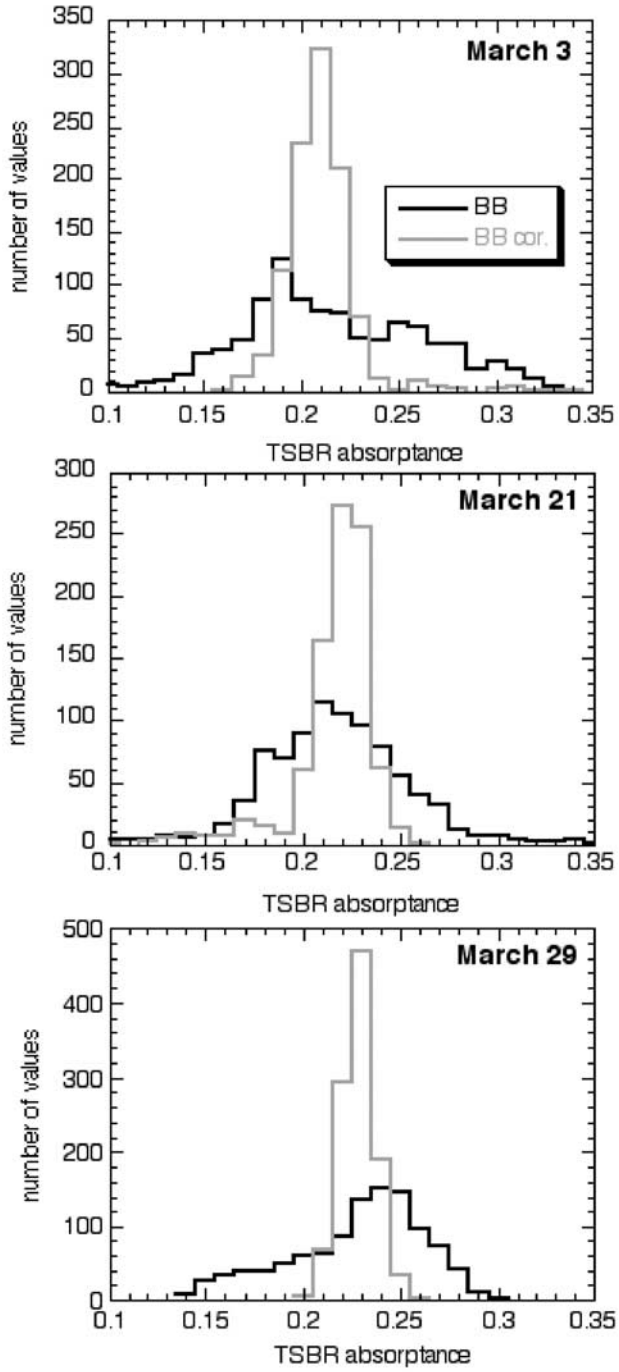

Figure 17. Histograms of the original and "corrected" TSBR absorptances of Figure 16.

much more than the upward flux; the latter results from contributions of reflected radiation from a far larger area of the cloud below. This is confirmed by inspection of the TSBR and CM22 upward and downward fluxes (not shown). If the surface fluxes are relatively insensitive to the upper cloud (as we expect them to be) the absorptance drops mostly in response to the drop in the Otter net flux. The magnitude of the drop depends on the details of the sensitivity of each instrument to reflected (upward) radiation from the outer edges of its field of view and the extent of time averaging in the measurements.

[29] For 29 March, the correction by (4) works fine throughout the entire data set, producing a distinctively flat absorptance time series (Figure 16c). The more uniform nature of the cloud produces unambiguous correlations between 500 nm and broadband absorptance (Figure 15c), resulting in the removal of most of the artificial features of the time series by (4). In other words, the variability in the original 29 March broadband absorptance time series (Figure 3) is largely due to 3-D and collocation effects and not a manifestation of the natural variability of the cloud (column) absorption. Similar to Figure 14, Figure 17 shows histograms of the absorptance time series before and after the correction by (4). The narrower histograms of corrected absorptance indicate a range of plausible "true" absorptance (defined by the boundaries of the main body of the histogram) that is $\sim$0.18–0.25 for 3 March and $\sim$0.20–0.25 for the other two days.

5. Summary and Discussion

[30] We have analyzed a wide range of ARESE II measurements in order to establish whether robust estimates of cloud broadband shortwave absorptance can be made. Our approach was to examine interinstrument differences, consistency of broadband and visible measurements, and adequacy of sampling. Our main finding is that of the three "best" overcast days of ARESE II, only one (29 March 2000) seems to satisfy the three most important requirements of an ideal ARESE II cloud system [*Ellingson and Tooman*, 1999], i.e., that it is thick, overcast (extensive), and horizontally homogeneous. These requirements help overcome the sampling limitations of the experiment stemming from the availability of a single aircraft. The 3 March cloud deck, as revealed by photographs taken by the Otter does occasionally present patches of clear sky, and is not thick enough, i.e., it seems to fail at least two out of three conditions. Moreover, the greater distance of the Twin Otter from the cloud top amplifies the averaging effects of the large field of view on the upward (reflected) fluxes. The 21 March clouds are extensive and thick, but exhibit a complex structure, thus failing the requirement of homogeneity. As a result, the degree to which the grand average broadband absorptance approaches the true average cloud absorptance for these two days cannot be assessed with the same confidence as for 29 March, when clouds satisfy all three requirements. However, careful analysis of 21 March demonstrates that data for that day were of better quality than for 3 March and can be retained for quantitative analysis that leads to important findings. A number of data analysis methods, such as cumulative averaging, conditional sampling, and point-by-point removal of horizontal flux/sampling artifacts are quite successful for 29 March as well as 21 March.

[31] Some specific highlights of our analysis are the following:

1. Broadband (uncorrected) absorptance for the three overcast ARESE II days is $\sim$0.21–0.22 for TSBR. The 29 March value of 0.22 is the most robust, followed by 21 March, while for 3 March the averaging may not be sufficient for the value to be considered reliable. In terms of W m^{-2}, the largest value of TSBR broadband absorbed flux occurs on 29 March, 231 W m^{-2} (partially a solar angle effect), while values for 3 and 21 March, were 197 and 211

W m^{-2}, respectively. These agree well with the values reported by *Powell et al.* [2001] and Ackerman et al. (submitted manuscript, 2002).

2. On 3 March, a systematically smaller absorptance was inferred from CM21 and CM22 compared to TSBR. It is due to the smaller downwelling and larger upwelling Twin Otter fluxes for the Kipp & Zonen instruments. The reason for the disagreement in the aircraft fluxes is unknown, although one can speculate that for the downwelling component differences in correcting for instrument mounting and navigational effects play an important role.

3. Conditional sampling cannot be applied on 3 March because narrowband visible absorptances are too high to be physically explained, especially in view of the generally smaller broadband absorptance for that day, and show an upward trend with time. Despite the sampling nature of a single aircraft experiment, conditional sampling *can* be applied, however, for 21 and 29 March when 500 nm absorptances are within the expected physical bounds and follow the variability of their broadband counterparts. Corrections à la *Cess et al.* [1999] seem also to be quite successful despite the general lack of collocation, because of the good correlation between broadband and narrowband visible absorptances. Histograms of corrected broadband absorptances from the two methods suggest that values outside the range 0.18–0.26 are most likely contaminated by horizontal flux and sampling effects.

4. The ARESE II sampling strategy can create fictitious correlations between short time averages of MWR LWP and apparent absorptances. This is due to the much stronger correlations of surface net fluxes with LWP compared to Twin Otter net flux and LWP correlations. Grand means of absorptance and LWP are not correlated, even when only collocated measurements are considered.

5. Clouds above the aircraft affect instantaneous estimates of absorptance due to their disproportionate effect on upwelling and downwelling fluxes. This is because the aircraft flies too far above the top of the lower cloud.

[32] From the above we conclude that although much progress in the understanding of ARESE II measurements has been made, further investigation of remaining unexplained discrepancies and their relationship to the properties of the cloud systems and/or the shortcomings of the experimental design is needed. From our perspective, it is particularly important to understand interinstrument differences of narrowband visible fluxes (something beyond the scope of the present study) and their relationship to broadband fluxes. Reconstruction of the cloud fields from observations and associated 3-D radiative transfer modeling will be very useful for this purpose.

[33] **Acknowledgments.** Data were obtained from the Atmospheric Radiation Measurement (ARM) Program sponsored by the U.S. Department of Energy, Office of Energy Research, Office of Health and Environmental Research, Environmental Sciences Division. We would like to thank S. Asano, P. Pilewskie, T. P. Tooman, and F. Valero for providing us information about the instruments they operated during ARESE II and the respective data streams. We benefited from discussions with T. Ackerman, A. Davis, R. Ellingson, R. Marchand, W. O'Hirok, P. Pilewskie, F. Valero, G. Wen, and W. Wiscombe. This research was supported by the Office of Biological and Environmental Research of the U.S. Department of Energy (under grant DE-AI02-00ER62939) as part of the ARM Program and by NASA grant NAG5-11631.

References

Ackerman, S. A., and S. K. Cox, Aircraft observations of shortwave fractional absorptance of non-homogeneous clouds, *J. Appl. Meteorol.*, *20*, 1510–1515, 1980.

Cess, R. D., M. H. Zhang, Y. Zhou, X. Jing, and V. Dvortsov, Absorption of solar radiation by clouds: Interpretations of satellite, surface and aircraft measurements, *J. Geophys. Res.*, *101*, 23,299–23,309, 1996.

Cess, R. D., M. H. Zhang, F. P. J. Valero, S. K. Pope, A. Bucholtz, B. Bush, C. S. Zender, and J. Vitko, Absorption of solar radiation by the cloudy atmosphere: Further interpretation of collocated aircraft measurements, *J. Geophys. Res.*, *104*, 2059–2066, 1999.

Ellingson, R., and T. P. Tooman (Eds.), *Science and Experiment Plan for the Second Atmospheric Radiation Measurement Enhanced Shortwave Experiment*, 1999. (Available as http://armuav.ca.sandia.gov/science-plans/w2000.pdf).

Li, Z., A. P. Trishchenko, H. W. Barker, G. L. Stephens, and P. Partain, Analyses of Atmospheric Radiation Measurement (ARM) program's Enhanced Shortwave Experiment (ARESE) multiple data sets for studying cloud absorption, *J. Geophys. Res.*, *104*, 19,127–19,134, 1999.

Marshak, A., A. Davis, W. Wiscombe, and R. Cahalan, Inhomogeneity effects on cloud shortwave absorption: Two-aircraft simulations, *J. Geophys. Res.*, *102*, 16,619–16,637, 1997.

Marshak, A., W. J. Wiscombe, A. Davis, L. Oreopoulos, and R. F. Cahalan, On the removal of the effect of horizontal fluxes in two-aircraft measurements of cloud absorption, *Q. J. R. Meteorol. Soc.*, *125*, 2153–2170, 1999.

Michalsky, J., et al., Broadband shortwave calibration results from the Atmospheric Radiation Measurement Enhanced Shortwave Experiment II, *J. Geophys. Res.*, *107*, 4307, doi:10.1029/2001JD001231, 2002.

O'Hirok, W., C. Gautier, and P. Ricchiazzi, Spectral signature of column solar radiation absorption during the Atmospheric Radiation Measurements Enhanced Shortwave Experiment (ARESE), *J. Geophys. Res.*, *105*, 17,471–17,480, 2000.

Powell, D. M., R. T. Marchand, and T. P. Ackerman, An analysis of cloud absorption during ARESE II (Spring 2000), in *Proceedings of 11th ARM Science Team Meeting*, 2001. (Available as http://www.arm.gov/docs/documents/technical/conf_0103/powell-dm.pdf).

Stephens, G. L., R. F. McCoy, R. B. McCoy, P. Gabriel, P. Partain, and S. D. Miller, A multipurpose Scanning Spectral Polarimeter (SSP): Instrument description and sample results, *J. Atmos. Oceanic Technol.*, *17*, 616–627, 2000.

Titov, G. A., Radiative horizontal transport and absorption in stratocumulus clouds, *J. Atmos. Sci.*, *55*, 2549–2560, 1998.

Valero, F. P. J., W. J. Y. Gore, and P. M. Giver, Radiative flux measurements in the troposphere, *Appl. Opt.*, *21*(5), 831–838, 1982.

Valero, F. P. J., T. P. Ackerman, and W. J. Y. Gore, The effects of the Arctic haze as determined from airborne radiometric measurements during AGASP II, *J. Atmos. Chem.*, *9*, 225–244, 1989.

Valero, F. P. J., R. D. Cess, M. Zhang, S. K. Pope, A. Bucholtz, B. C. Bush, and J. Vitko Jr., Absorption of solar radiation by the cloudy atmosphere: Interpretations of collocated aircraft measurement, *J. Geophys. Res.*, *102*, 29,917–29,927, 1997a.

Valero, F. P. J., A. Bucholtz, B. C. Bush, S. K. Pope, W. D. Collins, and P. Flatau, Atmospheric Radiation Measurements Enhanced Shortwave Experiment (ARESE): Experimental and data details, *J. Geophys. Res.*, *102*, 29,929–29,937, 1997b.

Valero, F. P. J., P. Minnis, S. K. Pope, A. Bucholtz, B. C. Bush, D. R. Doelling, W. L. Smith Jr., and X. Dong, Absorption of solar radiation by the atmosphere as determined using satellite, aircraft, and surface data during the Atmospheric Radiation Measurement Enhanced Shortwave Experiment (ARESE), *J. Geophys. Res.*, *105*, 4743–4758, 2000.

Valero, F. P. J., S. K. Pope, B. C. Bush, Q. Nguyen, D. Marsden, R. D. Cess, A. S. Leitner, A. Bucholtz, and P. M. Udelhofen, The absorption of solar radiation by the clear and cloudy atmosphere during the Atmospheric Radiation Measurements Enhanced Shortwave Experiments (ARESE) I and II: Observations and models, *J. Geophys. Res.*, *107*, doi:10.1029/2001JD001384, in press, 2003.

Zender, C. S., B. C. Bush, S. K. Pope, A. Bucholtz, W. D. Collins, J. T. Kiehl, F. P. J. Valero, and J. Vitko Jr., Atmospheric absorption during the Atmospheric Radiation Measurement (ARM) Enhanced Shortwave Experiment (ARESE), *J. Geophys. Res.*, *102*, 29,901–29,915, 1997.

R. F. Cahalan, Climate and Radiation Branch, National Aeronautics and Space Administration (NASA) Goddard Space Flight Center, Greenbelt, MD, USA.

A. Marshak and L. Oreopoulos, Joint Center for Earth Systems Technology, University of Maryland Baltimore County (UMBC), Baltimore, MD, USA. (lazaros@climate.gsfc.nasa.gov)